ELSEVIER

Coordination Chemistry Reviews
149 (1996) 367–400

COORDINATION CHEMISTRY REVIEWS

The distribution of aluminium in the Earth: from cosmogenesis to Sial evolution

Giancarlo Favero [a], Piergiorgio Jobstraibizer [b]

[a] *Università di Padova, Dipartimento di Chimica Inorganica, Metallorganica ed Analitica, via Marzolo 1, 35131 Padova, Italy*

[b] *Università di Padova, Dipartimento di Mineralogia e Petrologia, Corso Garibaldi 37, 35137 Padova, Italy*

Received 14 April 1995; in revised form 20 October 1995

Contents

Abstract

In this review the present distribution of aluminium in the Earth crust is discussed historically, starting from the origin of this element in cosmic nucleosynthesis processes and following its fate during the formation of the Solar System, the origin of the Earth, the segregation of siderophile–chalcophile from lithophile elements, the extraction of crustal material from the primitive fertile mantle and the subsequent redistribution of aluminium in sedimentary rocks and in the hydrosphere, which both are a peculiar feature of our planet, intimately connected with the presence of life.

Keywords: Aluminium; Cosmogenesis; Geology

1. Introduction

Among the 92 elements of the Periodic Table only ^{43}Tc and ^{61}Pm are not present in naturally occurring materials, while the remaining 90 have all been found in terrestrial as well as in extraterrestrial materials, such as meteorites and lunar soil.

The distribution and concentration of elements in the Earth as a whole is widely variable: as an instance, aluminium is completely absent from certain minerals and is an essential component in others. Its average concentration in the crust (about 8%), is surpassed only by that of oxygen and silicon. For this, the acronym Sial (silicon, aluminium) is used to characterise the chemistry of the crust, in contrast with the mantle acronym Sima (silicon, magnesium) used to outline its magnesium silicates composition.

In the underlying mantle, aluminium takes the fifth place after oxygen, silicon, magnesium, and iron, with an average concentration four times lesser than in the crust. As the mass of the crust is negligible with respect to the mantle (0.4% vs. 68% of the total Earth mass), and as aluminium is thought to be absent from the nucleus (31% of the total mass), about 1/40 of the aluminium of the whole Earth is present in the crust.

Was the inhomogeneous distribution of Al originated during the accretion of the planet or was it the result of succeeding transformations? In the latter case, what are the processes responsible for the partition of Al (and of the other elements) between crust and mantle reservoirs? When and how were the existing structural and compositional relationships between the two reservoirs defined? Did they exist when life appeared? Did they condition its evolution? As the chemistry of the crust and biological phenomena are peculiar to our planet, which relationships among the elemental abundance in the Earth crust do exist in the meteorites and in the soil of other planets? Do these abundances depend on the way in which the Solar System was formed 4.6 billion years ago or, on the contrary, are they determined only by the pool of elements formed in the time between the Big Bang and the birth of Solar System?

In the following we will try to give an answer to these questions, by outlining the pre terrestrial and terrestrial history of aluminium and of the other elements.

The period of pre-terrestrial history concerning the formation, the stability and cosmic abundance of elements is related to the thermodynamic conditions of various sites of nucleosynthesis (cosmochemistry).

The period of terrestrial history concerning the distribution and the behaviour of the elements is governed by their electronic configuration and by the thermodynamic conditions which prevailed during the condensation of matter from the solar nebula and its accumulation in microaggregates, in planetesimals, in protoplanetary embryos and finally in planets. The principles of geochemistry and the ongoing progress in all fields of Earth sciences allow us to follow the behaviour of aluminium and of the other elements in the terrestrial scenario, continuously sustained by solar energy and internal heat, still effective after 4.6 billion years.

2. Cosmochemistry

2.1. Cosmological nucleosynthesis

In recent years major progress has been made in understanding the origin of the chemical elements. After the pioneering work of Burbidge, Fowler and Hoyle and of Cameron, a self-consistent astrophysical scenario has been depicted by the efforts of Reeves and his co-workers and a few other groups.

Our Universe had a hot origin in the hypothesis of the socalled Big Bang, about 15 billion years ago. This hypothesis finds experimental evidence in three observable quantities. First, the red-shift in the spectra of remote galaxies reveals a cosmological expansion and implies that in a singular instant of the past the universe was a point-like structure of very high temperature and density. Second, the existence of a cosmic background of radiation, corresponding to a black body at 2.7 K, is the red-shifted trace of a very hot primordial stage of evolution. Finally, the high helium cosmic abundance is unexplainable without a primeval nucleosynthesis which generated this element during a hot phase.

A proposed scenario is the following. In the very early stages of the Universe ($t \ll 1$ s) the temperature was so high ($T \ll 10^{10}$ K) that matter and energy formed a hot, dense and rapidly expanding fireball. The matter existed in phases composed of exotic particles: mesons, quarks, gluons, etc., in equilibrium with energy. Only when the temperature lowered to about 10^{10} K, a few seconds after the Big Bang, the Universe consisted of photons, neutrinos, electrons, neutrons and protons. The synthesis of more complex nuclei would be impossible at such high temperatures, but the primordial gas was undergoing a steady cooling by adiabatically expanding. Thus, the combination of neutrons and protons became rapidly possible under the influence of the attractive nuclear force.

When the temperature dropped to about 10^9 K, a few minutes after the Big Bang, a series of neutron and proton capture reactions took place producing ^{2}H, ^{3}H, ^{3}He, ^{4}He, ^{7}Li and ^{7}Be. The formation of heavier nuclei was prevented by the extreme instability of those with mass number 5 or 8, and by the rapid cooling due to the steady expansion. After about three minutes the temperature was so low that nuclear reactions were no longer possible. The neutrons existing at this time decayed as follows:

$$n \rightarrow {}^1\mathrm{H} + \mathrm{e} + \nu$$

Thus, cosmological nucleosynthesis during the Big Bang produced primarily ^{1}H and ^{4}He, along with trace amounts of deuterium, ^{3}He, ^{7}Li and ^{7}Be. Beyond this phase the nucleosynthesis was no longer possible due to the decreasing temperature and particles' density, owing to the continued expansion.

A few hundred million years after the Big Bang, when the temperature cooled below 10^4 K, electrons were captured and atoms of H, He, Li and Be could form. The light flash released at this stage, red-shifted by the continued expansion, is actually observable as the cosmic background radiation the frequency distribution of which is the same of that emitted by a 2.7 K black body.

2.2. Stellar evolution

Matter in the expanding Universe underwent small temperature and density fluctuations, recently observed in the black body radiation cosmic background by COBE experiments. The attractive force of gravity, acting from regions of higher-than-average density produced substantial concentrations of matter in isolated regions of the space. This process represented the beginning of galaxy and star formation, a new site for synthesising new elements.

Gas clouds collapsed from the Big Bang material to form embryonic stars, in which the gravitational compression produced internal heating. The star core reached a temperature around 10^6 K and density about 100 kg dm^{-3}, creating the conditions for a chain of nuclear fusion reactions which produce the energy needed to balance the star gravitational collapse. In fact, at these temperatures and densities the protons acquire sufficient kinetic energy to overcome the electric charge repulsion, and hydrogen burning can start.

The preferred reactions produced helium isotopes from proton fusion with deuterium, lithium and beryllium atoms, which were depleted in the cosmic matter and only later were slowly reformed by cosmic spallation of higher nuclei.

$$^2H(H,\gamma)^3He$$

$$^7Li(H,\gamma)^8Be$$

$$^7Be(H,\gamma)^8B$$

$$^8B \rightarrow {}^8Be + e + \nu(\text{very rapid})$$

$$^8Be \rightarrow 2^4He(\text{very rapid})$$

At higher temperature the proton–proton fusion followed.

$$^1H + {}^1H \rightarrow {}^2H + e^+ + \nu$$

$$^2H(^1H,\gamma)^3He$$

$$^3He + {}^3He \rightarrow {}^4He + 2^1H$$

or, in stars already containing these elements, the CNO catalysed bicycle. Most of the stars are believed to be running on one of these energy sources or on a combination thereof for most of their stable lifetime.

Once the core hydrogen fuel becomes scarce, the helium-rich core cannot sustain the star gaseous mass, which starts a new contraction phase which increases interior temperatures. Hydrogen burning then continues in a hot shell surrounding the core, causing the envelope of the star to expand greatly giving rise to the so-called red giant phase, while the core temperature and density continue to rise. Stars that do not contain sufficient mass to sustain more advanced stages of nuclear burning simply exhaust their hydrogen fuel and undergo no further evolution. They become tiny white dwarf stars which cool slowly to the cosmic temperature. If the starting mass of the star is sufficiently large, the helium core reaches temperature (10^8 K) and densities (10^5 kg dm^{-3}) at which coulomb repulsion can no longer inhibit the

fusion between helium nuclei. Unstable ^{8}Be nuclei form from binary collision of ^{4}He nuclei and a certain number (about 1 atom in 10^{10} at 10^{8} K) exist long enough to capture a third ^{4}He to form an excited state of ^{12}C, which stabilizes emitting γ rays. Under these conditions one ^{12}C nucleus may capture another helium nucleus to form ^{16}O: in fact the helium fusion phase in stars should result in comparable yields of ^{12}C and ^{16}O.

Because only a relatively small fraction (about 0.07%) of the mass is converted into energy during the helium burning, the star is not stabilised for a long time by this process. When the helium fuel is exhausted in the core, leaving essentially a mixture of ^{12}C and ^{16}O, gravitational collapse will again set in, increasing the core temperature to about 10^{9} K and the density to about 5×10^{5} kg dm^{-3}. The various nuclear processes which can occur in successive time periods in the stellar core actually may all be occurring at the same time in different shells of an evolved star. An explosive nucleosynthesis can then take place originating the so called Supernova event (Fig. 1).

In the carbon–oxygen core just described carbon and oxygen burning will produce the following nuclear reaction series.

$^{12}C(^{12}C,^{4}He)^{20}Ne$ (ca. 50%)

$^{12}C(^{12}C,^{1}H)^{23}Na$ (ca. 50%)

$^{12}C(^{12}C,n)^{23}Mg$ (few%)

$^{12}C(^{12}C,\gamma)^{24}Mg$ (<1%)

$^{12}C(^{16}O,^{4}He)^{24}Mg$

$^{20}Ne(\alpha,\gamma)^{24}Mg$

with a new supply of α particles, protons and a few neutrons. Then the following nuclear reactions can occur.

$^{24}Mg(^{4}He,^{1}H)^{27}Al$

$^{24}Mg(n,\gamma)^{25}Mg$

$^{25}Mg(^{1}H,\gamma)^{26}Al \rightarrow {}^{26}Mg + e^{+} + \nu$

$^{26}Mg(^{1}H,\gamma)^{27}Al$

Only the isotope ^{27}Al is stable, while ^{26}Al is radioactive, in agreement with the odd–odd rule, and undergoes a β^{+} decay producing ^{26}Mg, with a lifetime of 7.05×10^{5} y. Four astrophysical environments have been suggested for the reaction $^{25}Mg(^{1}H,\gamma)^{26}Al$: (a) hydrostatic core hydrogen burning in stars with internal temperature higher than 4×10^{7} K, i.e. stars having mass higher than thirty solar masses, which eject ^{26}Al by strong stellar winds during the so-called Wolf-Rayet phase; (b) hydrostatic shell hydrogen burning at temperatures higher than 9×10^{7} K during the asymptotic giant branch phase; (c) explosive hydrogen burning at temperatures around $2–4 \times 10^{11}$ K during Nova explosion; (d) hydrostatic or explosive ^{12}C- or ^{20}Ne-burning in massive stars, ending their evolution as Supernovae. ^{26}Mg derived

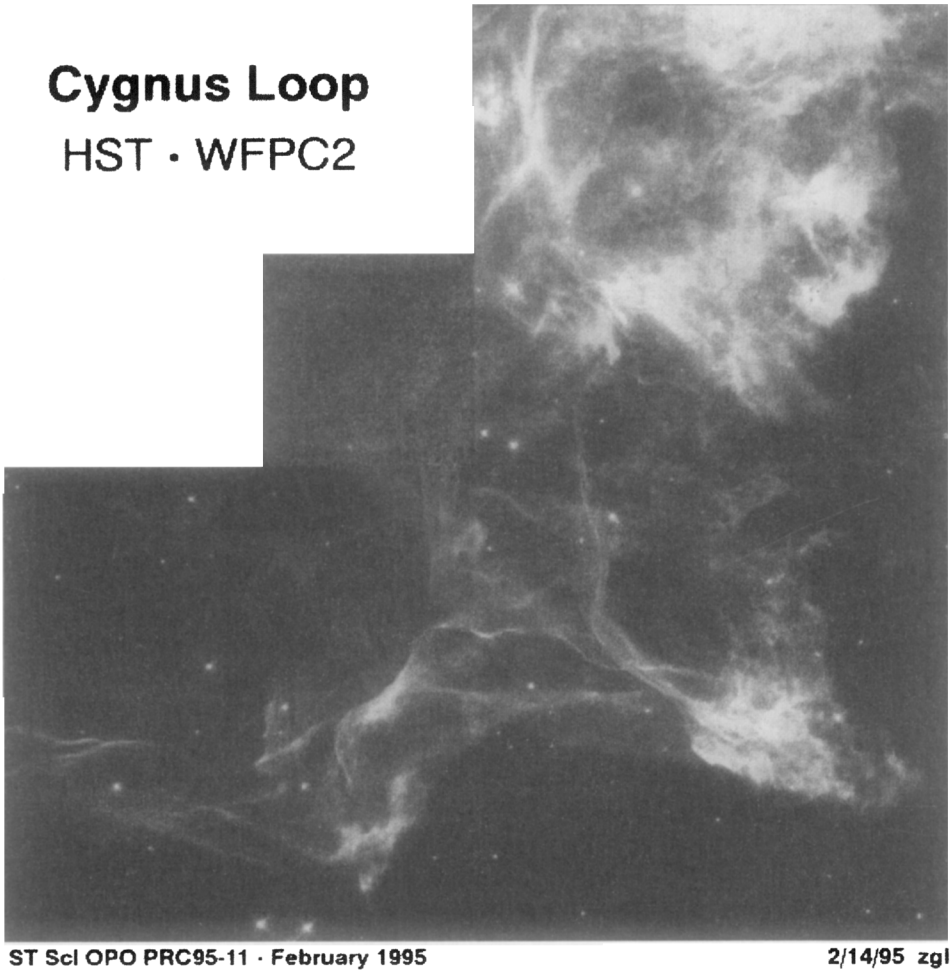

Fig. 1. View of a small portion of the Cygnus Loop, the expanding blastwave from a Supernova explosion which occurred about 1.5×10^4 years ago, 2500 light years from the Earth. The observations of Supernova 1987A confirmed that in these events an explosive nucleosynthesis occurs. The color is produced by composing three different images taken with the Wide Field and Planetary Camera 2 of Hubble telescope. Blue shows emission from O^{2+}, red shows emission from S^+ and green shows emission from H atoms.

from ^{26}Al has been detected in meteorites (chondrites): for an exaustive review on ^{26}Al cosmic distribution see MacPherson et al. [1].

Matter containing the newly synthesised aluminium isotopes is transported from the core or from the burning shell to the surface of the star by convection and finally to the interstellar medium by strong plasma winds, which can blow at 400–1000 km s^{-1}, or by the Novae and Supernovae exploding envelopes, expanding at 10^3–10^4 km s^{-1}. Less than 5 billion years ago, a particular cloud of interstellar medium enriched with the elements produced during 10 billion years of stellar evolution and

with those freshly synthesised during the explosion of a nearby Supernova, undergo a complex series of events starting with gravitational collapse and ending with the birth of our Sun and planets: between them, the Earth.

2.3. Formation of the Solar System

We start with a spheroidal mass of initially cold interstellar matter that is rotating and collapsing, undergoing intense heating due to the release of gravitational energy. The central region of the cloud rapidly collapsed, in about 10^5 years, forming a star containing nearly all the starting mass. A minor but important part of the material failed to fall into the Sun because of the centrifugal force which developed at the equator of the collapsing and rotating cloud. This matter settled rapidly forming a flat disc around the Sun. While the outer, lower density regions of the contracting nebular disc may have remained quite cold, closer to the Sun and to the equatorial plane the material was completely evaporated at temperatures higher than 2000 K.

The composition of the atomic gas is illustrated in Fig. 2, but can be simply accounted for by the following figures: nearly 98% in mass is represented by hydrogen

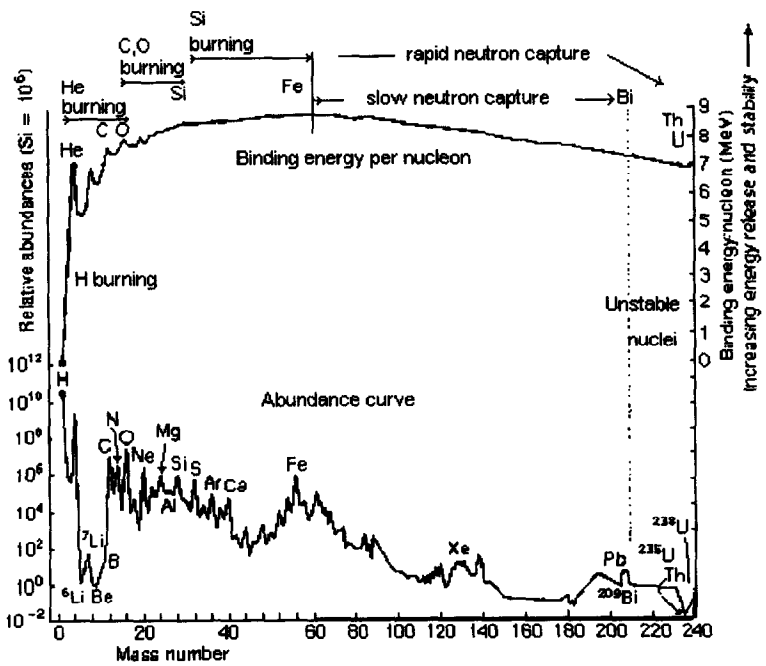

Fig. 2. Abundance of elements and their isotopes (lower curve) compared with the stability (binding energy per nucleon, upper curve) of their nuclei. The nucleosynthetic routes are schematically reported. (After Ref. [11], modified).

(74%) and helium (24%); carbon, nitrogen, oxygen and neon amount to 1.3%; magnesium, silicon, iron and aluminium, nearly in the same amount, account for a 0.3%; sodium, sulphur, potassium and calcium are an order of magnitude lower; all the remaining elements are comprised in a small 0.4%.

Owing to the low gas pressure ($1–10^4$ Pa) the cooling of the atomic material led to a gradual condensation of mineral compounds. Defining compounds that condense above 1200 K as refractory, in contrast with those that condense at lower temperatures and are termed volatile, we can apply to the elements the following categories: highly refractory (Al, Ca, Ti), moderately refractory (Mg, Fe, Si), moderately volatile (Na, K, S) and highly volatile or gaseous (H, He, C, N, Ne) elements. Therefore, aluminium is the most abundant of the highly refractory elements. It will be the first to condense out from the preplanetary nebula and will occupy an important role in the chemistry of all the solid bodies of the Solar System.

The main processes governing planetary chemistry took place during the first 100 million years following the nearby Supernova explosion. Within the first $10^4–10^5$ years the gravitational collapse of the initially cold preplanetary nebula caused a strong heating and a substantial vaporisation of the matter. Subsequent cooling allowed sub-micron sized dust grains to form by recondensation of the atomic mixture, following the order of decreasing molecular volatility. Average dust grain composition varied radially across the nebula because of outwards decreasing pressure — controlling for example the iron/silicate ratio — and temperature — controlling the volatile/refractory element ratios. A so-called snow line existed at about 600–700 million km from the Sun: first water, then ammonia and finally methane ices condensed together with the dust and accreted in volatile-rich grains, whose density lowered going outwards in the pre-planetary nebula. Strong T-Tauri winds blowing from the adult Sun removed over 90% of the material potentially involved in planetary formation, but still in the form of uncondensed gases.

Volatile and dust grains accreted together giving the planetesimals, the first solid bodies existing in the proto-planetary nebula, whose formation caused a progressive perturbation in the formerly ordered circular motion of the matter around the Sun. The composition of the planetesimals resulted regularly differentiated and related to the regions of the Solar System where they were born: mainly refractory in the inner regions, near the Sun, then metallic and chondritic as one recedes from the Sun, and finally mainly icy in nature. The likely processes that governed the chemical fractionation were the decreasing temperature and pressure away from the Sun. A marked pressure variation over the width of the asteroid belt is suggested by the density variation in the population of chondritic meteorites. The iron/silicate fractionation which is evident in their analysis (going from the low value 0.5–0.6 in the L and LL types, to the high 0.8 value in H type) is accompanied by the similar fractionation of other metallic elements and by the depletion of volatile compounds.

The dimensions of the condensed bodies ranged from a few millimetres to a few meters and the chance of collision between them increased with the extensive modification of their orbits from circular to elliptic. Planetesimal encounters were mainly cohesive in nature, leading to the gravitational accretion of planetary embryos, a process which lasted only a few thousand years. When the masses of the planetary

embryos reached a few percent of their present value a systematic segregation of the constituents started as the accretional and radioactive heating raised internal temperatures high enough for extensive melting to occur. Liquid drops began to develop, initially close to the surface where impact energy was most effectively converted into heat, then precipitated towards the planet interior. In this phase of core formation, with separation of denser metallic components from the lighter alumino silicates, further gravitational energy was converted into heat and the interior of the larger embryos became chemically differentiated. Small embryos never became extensively melted and their interiors resulted less differentiated. This picture is presently frozen in the different types of meteorites whose various composition can well reflect the fragmentation of internally differentiated bodies or nearly undifferentiated ones.

In differentiated planets and meteorites the elements were sorted into groups according to their electronegativities. Highly electronegative siderophile elements (Ir, Pt, Au), tended to be metallic. Chalcophile elements, with intermediate electronegativity and marked tendency to form covalent bonds (Co, Cu, Zn, Pb), concentrated as sulphides. Lithophile elements, which have low electronegativity and form mainly ionic compounds, (Na, K, Mg, Ca, Al) occurred in oxides and silicates. Atmophile elements (H, C, N, O and noble gases) remained gaseous in the conditions prevailing at the surface of some planets (Venus, Earth, Mars).

Turning our attention to the Earth, during the last stages of gravitational accretion of the planet siderophile and chalcophile elements separated into the core, dominated by iron; sodium, potassium, magnesium, calcium and aluminium substituted iron in the lithophile silicate mantle, according to the following. The best estimate of the overall Earth chemical composition is given in Fig. 3, where appear the seven most abundant elements which account for the 97% of its mass. Referring to the atomic proportions, we can account for initial formation of SiO_4^{4-}, followed by the rapid uptake of Ca^{2+}, Mg^{2+} and Al^{3+} for silicate formation (olivine, pyroxene). As a result three or four cations combine with four to six oxygen anions, so that more oxygen atoms than cationforming atoms are needed to produce neutral compounds. This fact suggests that some iron could have been combined with the available sulphur, leaving the remaining in the metallic form: thus iron atoms joined the siderophile elements in the Earth core.

Provided that the interior temperature of the increasing embryo is high enough for extensive melting, the combinations described result in three separate layers of increasing density with depth. The metallic inner core containing iron is surrounded by an outer core containing FeS over which the Mg–Fe silicate mantle is found. In the Earth the efficiency of this process has been high, but the separation is still not complete, leaving at the surface traces of sulphur, gold and platinum. There is little doubt, however, that aluminium, calcium and alkalis have been confined almost entirely to the light silicate external layer which forms the terrestrial crust. Comparison between element abundance in the solar atmosphere (representing the original solar nebula composition) and in the Earth's continental crust, reported in Fig. 4, confirms that chalcophile, siderophile elements and iron are depleted, while aluminium, alkalis and other elements are enriched in the planetary crust.

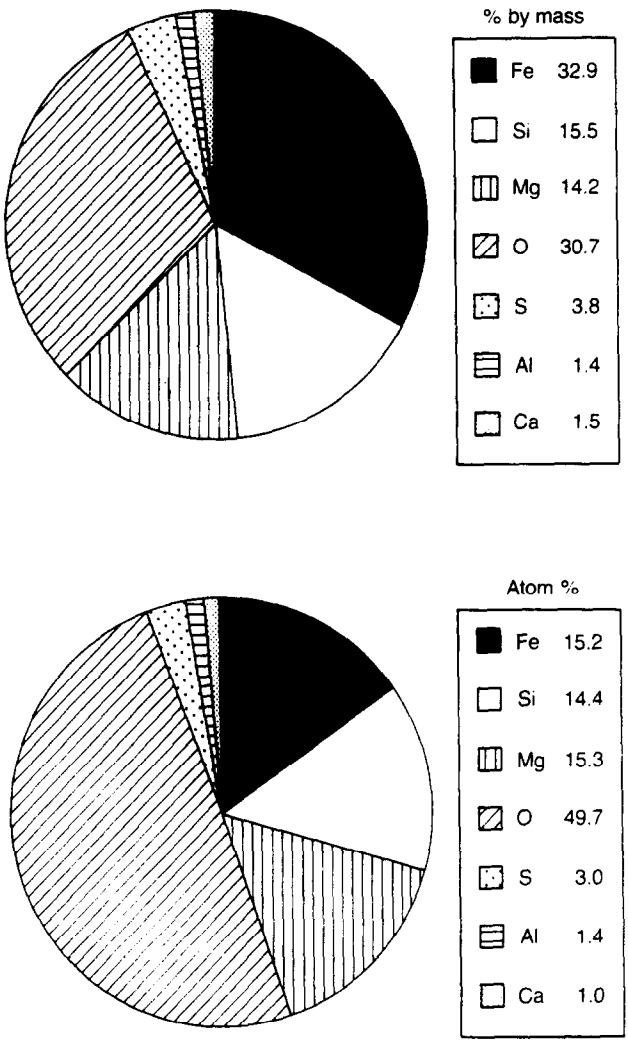

Fig. 3. Relative amounts by mass (upper) and by number of atoms (lower) of the seven elements more abundant on the Earth. (After Ref. [11].)

3. Geochemistry

3.1. Layered structure of the Earth

To understand the distribution of the elements we need a knowledge of the structure and of the composition of the various parts of our planet as well as of the main geological processes which are operating.

The outer part of the planet, the so called Earth crust, is a solid shell, having a depth of a few kilometres under the oceans and some tens of kilometres in continental

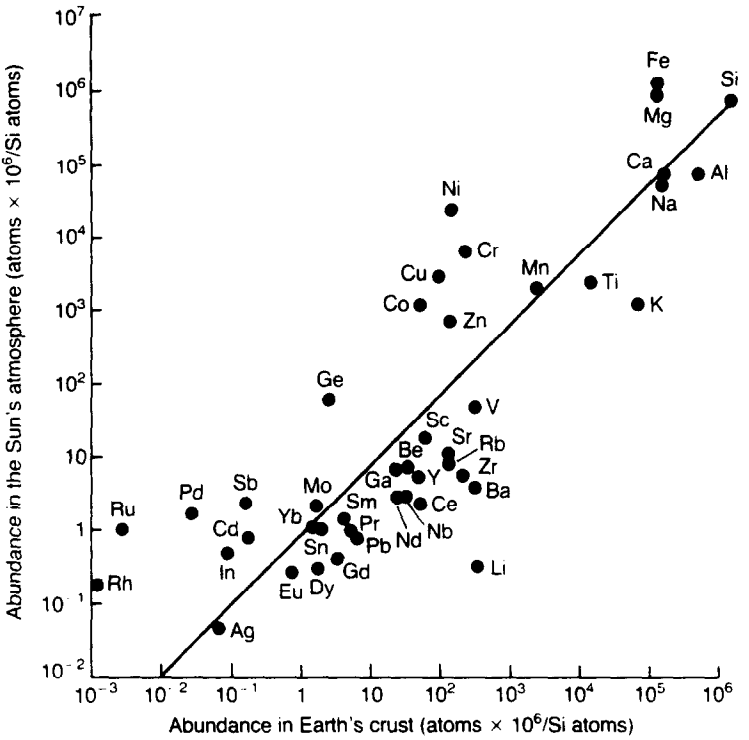

Fig. 4. Comparison between elemental abundances in the solar atmosphere and in the Earth continental crust. (After Ref. [11].)

areas, and comprising less than 1% of terrestrial mass and volume. The chemical composition of the crust, as well as the variety of structures and of geodynamic processes observed in it are obviously connected to the physico-chemical properties of deeper layers, inaccessible to direct sampling and observation. However, this inaccessibility is not an insuperable obstacle, and many kinds of information are contributed by astronomy, astrophysics, nuclear physics, planetary physics, geophysics, geochemistry and geology.

Cross controls and constraints of these disciplines permits one to obtain a close approximation to the plausible constitution of the Earth. A fundamental contribution to our knowledge of the inside of the Earth comes from the seismology. The analysis of seismic waves, travelling at different velocities through the planet and emerging far from their sources, gives detailed information on the physical properties of the whole terrestrial body. Among them, temperature and density are relevant to unravel the structure–composition relations.

The measurement of the acceleration due to gravity shows that the average Earth density is 5.52 g cm^{-3}: as the density of surface rocks is less than 3 g cm^{-3}, the density of the inner part of the Earth must be higher than 6 g cm^{-3}. The increase

in temperature with depth is well known, and witnessed by phenomena as volcanic eruptions.

Vertical profiles of density are recognisable from seismic profiles of P and S waves (Fig. 5) and from other constraints. P waves (or compressional waves) travel both in solid and in fluid media, while S waves (or shear waves) propagate only in solids, at a speed which is about one half of that of P waves. The speed of seismic waves depends on the square root of the elastic moduli/density ratio. As the two seismic

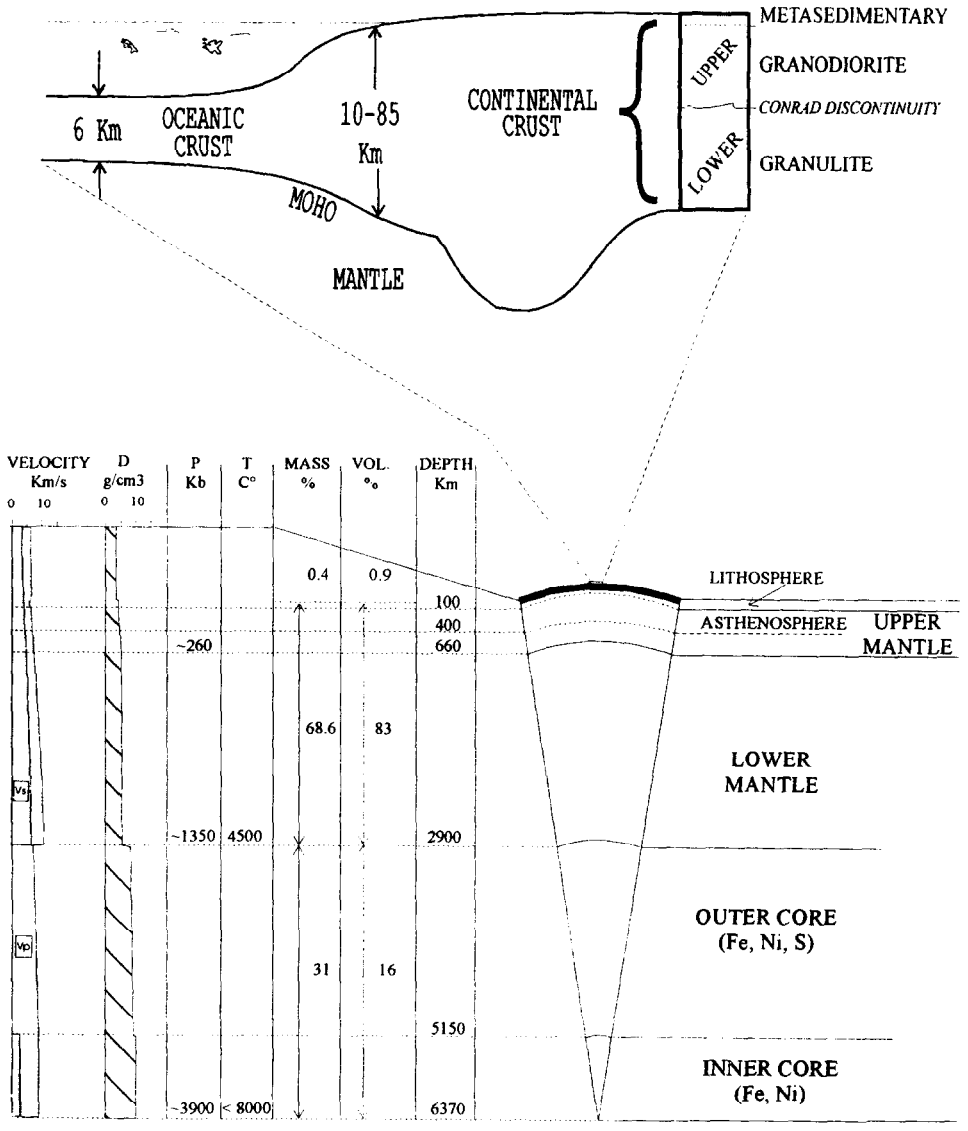

Fig. 5. Sector of the Earth with expanded crustal layer. Major physical and structural features are shown.

velocities depend upon three variables (compressibility, rigidity moduli and density) it is not possible to deduce how density varies with depth, in the absence of a third relationship. Reasonably, however, the density must increase with depth due to self compression and coherently with the nature of the medium. On the other hand, composition must be consistent with elemental abundancies (Fig. 3) and with the presence of solid matter in regions in which P and S waves propagate and of liquid matter in regions where S waves disappear.

In the velocity profiles of P and S waves three sharp changes are apparent: the first is the so called Mohorovicic discontinuity (or in short-form Moho), which is found at 6–7 km beneath oceanic floor and at an average depth of 30 km (with a range from 10 to 85 km) under the continental surface. This discontinuity is due to an allochemical transition, occurring in a belt a few kilometres thick, between the crust and the underlying solid mantle of different chemical composition. The second discontinuity, which is found at a depth of 2890 km, is marked by the disappearance of S waves and by an halving of the speed of P waves and indicates the transition between solid mantle and liquid nucleus. The reappearance of S waves, at a depth of 5155 km, indicates the transition between liquid outer core and solid inner core.

The assumption of an iron rich nucleus is consistent both with the temperature and density gradients shown in Fig. 5 and with the fact that in the nucleus a metallic conducting medium produces and maintains the magnetic field of the Earth. The abundance of Fe, Ni, and S is assumed as the result of the initial metallic segregation discussed previously. As there is no reason to suspect the presence of Al in the nucleus we will focus our attention on the state of the mantle and of the crust. Both regions are characterised by the existence of second order discontinuities at 2890 and 5155 km, less evident than first order ones, but very significant for the interpretation of the relationships between composition and structure.

3.2. *Aluminium in the mantle and in the oceanic crust*

As direct sampling and observation of the mantle are virtually impossible, the main sources of evidence on the nature of the mantle are indirect, and come from (a) the genesis and composition of chondrytic meteorites; (b) the chemical and mineralogical composition of rocks derived from subcrustal magmatic sources; (c) experimental petrology at pressures and temperatures similar to those prevailing in the mantle.

(a) The linkage to chondrites appears reasonable owing to the common origin of our planetary system, previously discussed; the kinship between bulk silicate Earth and chondrites is confirmed by the data in Table 1: the most abundant elements on the Earth are also the most abundant in chondrites, in which O, Si, Mg and Fe form the most abundant minerals olivine $(Mg, Fe)_2SiO_4$ and orthopyroxene $(Mg, Fe)_2Si_2O_6$, while Al and Ca form minerals as plagioclase ($CaAl_2Si_2O_8$; $NaAlSi_3O_8$) and clinopyroxenes or they can substitute for major elements in other minerals.

(b) The above mentioned minerals are found also in basalts of the oceanic and continental crust, although in different proportions (plagioclase is here the prevailing mineral). Basalt rocks can host small nodules formed mainly by olivine and orthopy-

Table 1
Chemical composition of mantle and crust materials

	1 Undepleted upper mantle	2 Olivine nodules	3 Lherzolite	4 Oceanic crust	5 Continental crust	6	7
					Bulk	Upper	Lower
SiO_2	46.2	42.5	45.3	50.0	58.9	64.2	54.4
TiO_2	0.2	0.0	0.2	1.4	0.8	0.6	1.0
Al_2O_3	4.7	0.5	3.6	17.0	16.2	16.3	16.1
FeO	7.7	7.1	7.3	9.9	8.1	5.8	10.6
MgO	35.5	49.5	40.3	8.0	4.5	2.6	6.3
CaO	4.4	0.3	3.0	10.8	7.1	4.6	8.5
Na_2O	0.4	0.1	0.3	2.6	3.0	3.4	2.8
K_2O	0.0	0.0	0.0	0.3	1.4	2.5	0.3

roxene and distinguishable according to their Al, Ca and Na contents among dunitic or harzburgitic nodules (low contents, number 2 in Table 1) and lherzolite-like nodules (high contents, number 3 in Table 1). A comparison between the chemical composition of nodules and that of basalts of the oceanic crust (number 4 in Table 1) suggests a kinship between basalts and lherzolite. In the hypothesis that basalts are derived from a magma produced by the partial melting of mantle nodules, those lacking of Al and Ca should be excluded as basaltic magma source, while lherzolitic nodules may be considered as parent material. Fig. 6 shows how a partial melting of lherzolitic material produces the selective extraction of Al, Ca, Na, Ti, ... so that the composition of the produced magma shifts towards that of basalt, while the

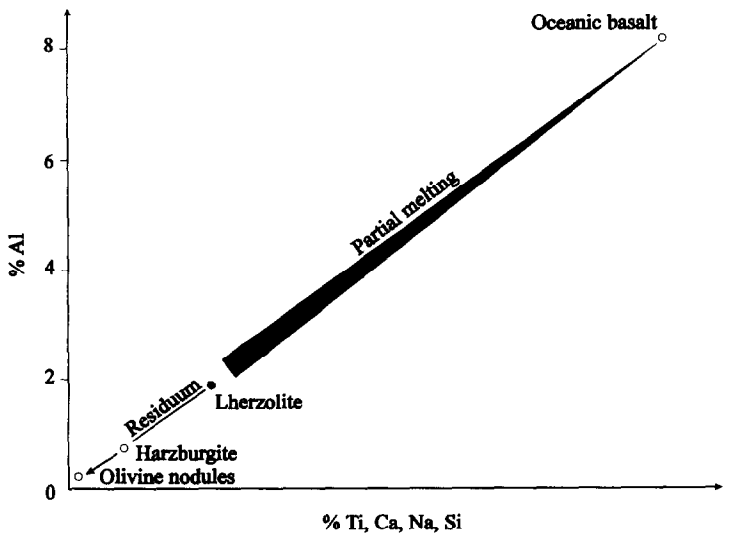

Fig. 6. Partial melting of fertile lherzolite in the upper mantle. The extration of fusible elements forming basaltic magmas leaves a refractory residuum of olivine nodules. (After Ref. [11], modified).

composition of the refractory residual shifts in the opposite direction, towards that of hazburgite and olivine nodules (number 2 in Table 1). Moreover, if Al_2O_3 and CaO were completely drained from the lherzolite and concentrated in the basalt, the data give a concentration factor of $15.0/3.6=4.2$ and $11.4/3.0=3.9$, respectively; conversely for MgO the factor is $11.0/40.3=0.27$. These values indicate a maximum limit of 25% on the degree of partial melting. A lesser degree of partial melting would give a different composition of both the melt and the residue, as proved by the existence of different types of basalt and of nodules. It is commonly believed that the degree of melting is generally low (<2%) but repeated in time according to a production–removal rhythm of low-viscosity melt.

Now, if crustal basalts are formed through a selective draining of elements released by fertile lherzolite in the mantle, several questions arise: there exists a proportion between the mass of basalts produced and that of depleted mantle. Are the physical properties of the depleted refractory mantle different from those of the fertile mantle? How does the mineralogical association of the mantle vary with seismical and thermal profiles? Where, when and why does partial melting takes place?

(c) Mineralogy and petrology give an answer to the above questions by subjecting a series of rocks to different temperature at same pressure (and vice versa). The products so obtained reveal for each sample the temperature at which melting begins; by repeating the processes at different pressures many points in the P–T space result and solidus line is drawn; similarly a liquidus line is obtained by joining the points where total melting is accomplished; partial melting, i.e. a mixture of crystals and liquid, occurs in temperature interval between solidus and liquidus. Coeteris paribus, the first melt to appear among a mineral assemblage derives from the mineral having the lower melting point; this is strongly depending on composition: for instance, in the isomorphic series of olivines, $(Mg,Fe)_2SiO_4$, the endmembers melt at 1890 °C (Mg) and at 1205 °C (Fe), respectively. Under anhydrous conditions the melting point increases with pressure, whereas under water saturated conditions, it decreases with pressures.

Fig. 7 shows the melting relationships and products of the same dry lherzolite in a P–T space of the upper mantle. Assuming an initial geothermal gradient of $11\,°C\,km^{-1}$, the first melt should appear at 1650 °C where the projected geotherm intersects the solidus line at 150 km depth. In real normal mantle, however, various thermal perturbations may produce variations on the geotherm slope and depress the melting points, thereby shifting to lower temperatures both solidus and liquidus lines. Common depressive factors are: volatiles release, decompression due to extensional stress, and rising higher temperature material in convective plumes.

In the subsolidus region of Fig. 7, the same lherzolite assumes different mineralogy according to the changing P–T conditions. At lower pressures (depth <25 km) olivine and orthopyroxene are the main phases with subordinate plagioclase and clinopyroxene.

At higher pressure (depth >25 km) the instability of plagioclase promotes the reaction

$$2(Mg,Fe)_2SiO_4 + CaAl_2Si_2O_8 \rightleftharpoons MgAl_2O_4 + (Ca,Mg,Fe)_2Si_2O_6 + (Mg,Fe)_2Si_2O_6$$

olivine plapioclase spinel clinopyroyene orthopyroxene

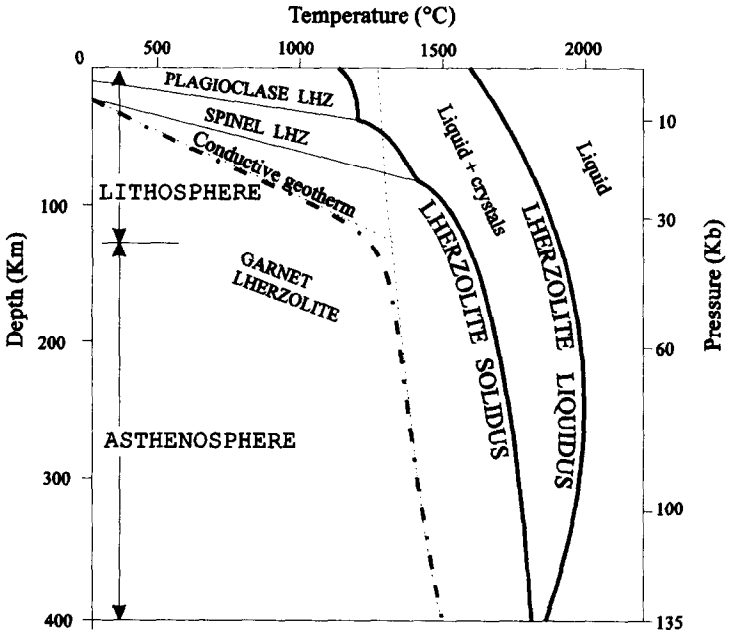

Fig. 7. Composition of lherzolitic mantle. Faint lines indicate boundaries between different mineralogical associations appropriate to P–T conditions. Heavy solid lines indicate dry solidus and liquidus curves. Composition of magmas resulting by partial melting depends on the mineralogy, degree of fusion and thermodynamic conditions. Variation of temperature with depth is rapid in the upper mantle where heat transfer is by conduction; more in depth, the geotherm follows the convective mantle adiabat. Geotherm and solidus curves can be deflected owing to release of volatiles, rising of hot low density mantle and decompression: thus the melting may initiate at lower temperature and minor depths than shown in figure. (After Ref. [11], simplified).

At still higher pressure, (depth >75 km) the instability of spinel promotes the reaction

$$2(Ca,Mg,Fe)_2Si_2O_6 + MgAl_2O_4 \rightleftharpoons CaMg_2Al_2Si_3O_{12} + (Mg,Fe)_2SiO_4$$

clinopyroxene spinel garnet olivine

It is worth mentioning that the above changes affect only a small fraction of the lherzolite mineralogy.

The association formed by: olivine ($\approx 60\%$), orthopyroxene ($\approx 20\%$), garnet plus a few omphacitic clinopyroxene ($\approx 7\%$) is stable down to transition zone (Figure 5) where reconstructive perturbation affecting olivine and orthopyroxene initiates at 400 km and accomplishes at 600 km; at this depth, garnet and clinopyroxene also suffer a severe structural modification. The seismic discontinuity at 660 km is due to the stabilisation of the denser and more closely packed $(Mg,Fe,Ca)SiO_3$ [perovskite] and Al_2O_3 [corundum] structures.

Summarising and focusing on the aluminium distribution through the mantle, at low pressure aluminium occupies the tetrahedral sites of the plagioclase lattice; at

higher pressures it assumes octahedral coordination in the more and more dense and closely packed structures of spinel, garnet, and corundum.

The partial melting of the lherzolitic mantle may occur at depths ranging from a few km beneath oceanic ridges (Fig. 8a) to 300 km. Beneath 100 km the production of melt decreases with increasing depth and it appears controlled by release of volatiles from hydrated minerals as flogopite $KMg_3[AlSi_3O_{10}(OH)_2]$. However, the rising of melt is unlikely to occur from levels deeper than 200 km, where the more compressible melt probably assumes a greater density than coexisting olivine–orthopyroxene, as suggested by negative P–T slope on the liquidus line at pressures greater than 70 kb (Fig. 7).

At depths less than ca. 100 km, major fractions of melt are promoted by rising hot plumes or by decompression linked to strong extensional stress as in ocean ridges. Regions beneath 10–20 km in oceanic areas and 50–60 km in other areas are

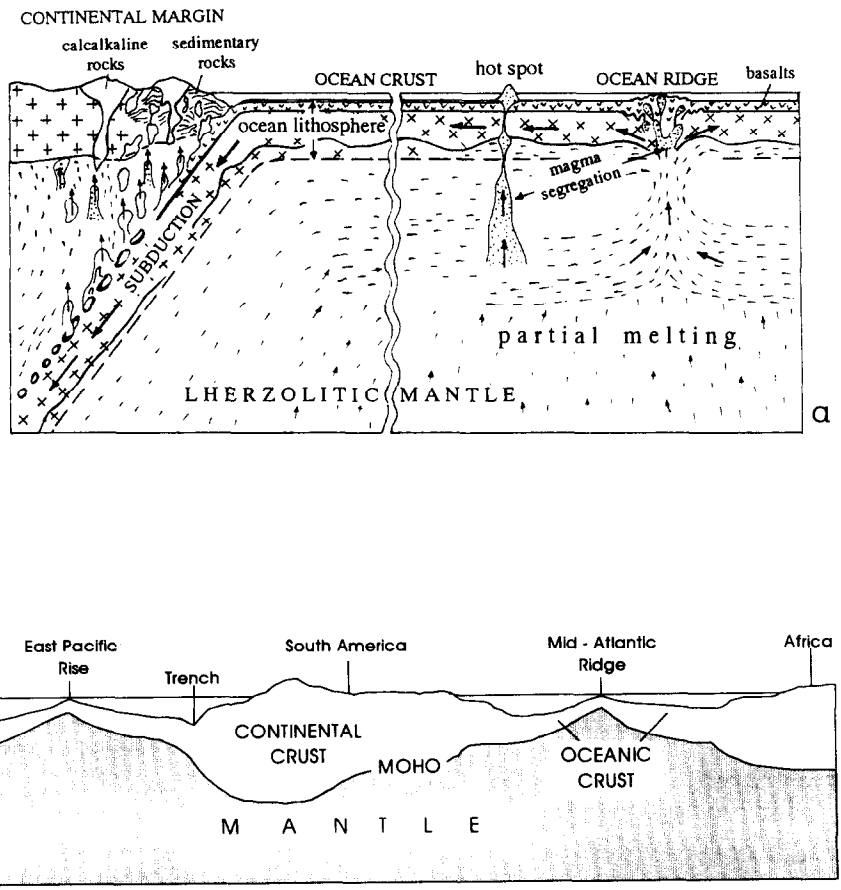

Fig. 8. (a) Picture of the main geodynamic processes of the crust and upper mantle according to the plate tectonic theory. (b) Relative thickness of oceanic and continental crust in a cross section from Africa to Pacific rise. (After Ref. [11], modified).

the main basaltic magma producers. The compositional data on the variability of basalts (and more or less depleted hosted nodules), integrated with considerations of fluid dynamic, indicate that basalt melts of low viscosity leave source region at small liquid fractions; so that repeated cycles of melt extraction are necessary to generate the resulting normal ocean basaltic crust 6–7 km thick. The mass of oceanic basalts requires that 10%–15 % of shallow mantle must have melt through a series of successive batches of small melt fractions (ca. 1%). These travel upwards at velocity of 5–10 cm per year, so requiring 10^5 to 10^6 years to arrive from sources 10–50 km deep.

The speed of magma ascent is similar to that ascertained for ocean-spreading; so that a large volume zone with melt fractions exists in the upper mantle, feeding oceanic crust at a rate of 20 km^3 per year. According to plate tectonic theory, oceanic plates are transient features: in a span of less than $1–2 \times 10^8$ years they plunge into the mantle and give rise to a subduction zone (Fig. 8a). Here, a progressive destruction of the oceanic plate does not simply cycle mantle material, but also separates chemical elements, so that the material returned to the mantle differs from that at its source region at the ocean ridge.

Ultimately, the thermal convection and extraction in small melt fractions from a well mixed regime at depth along the solidus (Fig. 7), has a major consequence the creation, movement and downwelling of plates and the chemical heterogeneisation of the mantle. The processes of basalt generation by partial melting and of plate subduction pose the question of how much depleted material then is in the upper mantle after billions of years of processing and to which extent and to which depth the upper mantle is depleted. Perhaps the same fertile lherzolite is slightly depleted compared with the undepleted upper mantle: in this sense are the minor contents of fusible elements Al, Ca, Na of the analysis number 3 with respect to the analysis number 1 of the Table 1 interpreted.

3.3. Aluminium in the continental crust

Present day crust growth is readily accounted for by volcanism in orogenic zones and island arcs where oceanic crust subduces into the mantle. There, conditions are favourable to production and rising of melts which generate calcalkaline rocks of plutonic and volcanic body of continental crust. (see left side of Fig. 8a) In other words, geological processes responsible for generating the continental crust operate on a scale which has involved much of the mantle and oceanic crust. This continental growth mechanism is thought efficient by 2.5 Ga (billion years) (post Archean) and account for about 20% of modern crust. The remaining about 70% was generated during pre Archean era (3.2–2.5 Ga). The most likely early crust on the Earth was basaltic or more basic (i.e. Mg rich), generated by partial melting within the solid mantle. Production of more sialic crust was a much less efficient process, although it has begun on a local scale at 3.8 Ga. Crustal growth is greatly concentrated in episodes of accelerate growth during the periods 3.8–3.5, 3.3–2.5 Ga and others. Possibly, about 50% of the continental crust was generated during 2.8–2.5 Ga. Periods of crustal growth were followed by rapid intracrustal melting and differentia-

tion into upper crust (enriched in incompatible, or hygromagmatophyle elements, i.e. the elements which during crystallisation and partial melting processes tend to concentrate in the liquid phase) and lower crust (depleted in incompatible elements).

The very large percentage of incompatible elements such as Ca, Rb, K, Th, REE (rare earth elements) in the continental crust indicates the processing of very large fractions of the mantle to produce the crust from 30%–50% of the mantle.

The memory of early events will be found only in minor part (ca. 1×10^6 km^2) of the crust, older than 2.7 Ga. The modern land area of continents covers 29% of the surface; but if the submerged continental areas are included, this figure rises to 41% (210×10^6 km^2). Continental crust prevails on oceanic crust both in volume (0.7% vs. 0.2%) and in mass (0.3% vs. 0.1% of whole Earth whose absolute mass is 6.10^{27}g). The pattern of continental crust thickness (Fig. 8b) mimics the main surface components (platforms, continental shields, folded mountains chains, etc.). Seismic data reveal a layered structure exemplified in Fig. 5: a thin top layer of metasedimentary rocks is underlined by a thick layer of eruptive and metamorphic rocks of an averaged granodioritic to tonalitic composition (number 6 in Table 1); the two layers form the upper crust. The seismic Conrad discontinuity separates the upper from the lower amphibolitic–granulitic crust (number 7 in Table 1). The proportions of upper and lower crust may differ significantly depending on geological history. More in general the top layer occupies less than 10% of the volume but ca. 75% of the extent of the upper crust.

To summarise, extraction of the present upper crustal composition (number 6 in Table 1) from the mantle made only minimal changes to the major element composition of the upper mantle (number 1 and 3 in Table 1). This is in strong contrast to the Moon, where the lunar highland crust comprises 10% of lunar volume and concentrated perhaps 50% of the Al content of the bulk Moon. By contrast, Al in the Earth crust is about 2.5% of the Al content of the bulk Earth. Among the planets in the inner Solar system, only the Earth produced an unique surface environment of granitoid composition. The underlying cause for this behaviour is probably the presence of liquid water at the surface of the Earth; water is essential for the production of granites, which so restrict their occurrence in large quantities to the Earth. It is interesting to note that water, essential for the evolution of life from the beginning, also plays a major role in the production of platforms above sea level, on which life has evolved to its present diversity.

3.3.1. Chemistry and mineralogy

The continental crust is by far more heterogeneous than the oceanic crust, both from the chemical and from the mineralogical standpoint. The genetic link between the two kinds of crust requires a comparative analysis between mineralogy and chemistry in both (number 4 and 5 in Table 1). The composition of the continental crust is obtained indirectly by evaluating the contributions (chemical and mineralogical contributions) of the (accessible) upper crust and of the (generally inaccessible) lower crust. The composition of bulk crust is hence model dependent, but it must meet the heat-flow constraints and must be capable of generating the upper crust

by intracrustal partial melting; it must also be derived from the mantle by reasonably common geological processes.

The validity of the current opinion that the bulk crustal composition is able to produce, by intracrustal melting, the presently observed granodioritic upper crust, is supported by the compositional relationships (of the data) reported in Table 1; the composition number 7 is obtained by combining composition number 5 (48%) and number 6 (44%); the remaining 8% is given by the composition (not shown) of the top layer of metasedimentary rocks, which is similar to composition number 6, but with a lower Si content and double the amount of Ca.

Formation of the upper crust entails a depletion of Ca, Mg, Fe and an enrichment in K, Na, Si (and also in incompatible elements as Rb, Th, Ba, etc.); surprisingly, only aluminium is not fractionated either by the oceanic crust, or by continental crusts, lower and upper: in fact, the concentration of Al_2O_3 is between 16 and 17% in the three regions. The interpretation of this behaviour requires an examination of the mineralogical transformations involved in the chain of petrogenetic processes. In the following, we will focus our attention on the mineralogy of aluminium.

3.3.2. The distribution of aluminium in crystalline rocks

The solid part of the terrestrial crust is formed by rocks, defined as aggregates of one or more minerals; a mineral is in turn defined as a naturally occurring inorganic material, having a definite composition. The number of minerals known 30 years ago was 1700 and has at the present increased to about 3500 [2]; this is a surprisingly low number, taking into account the number of chemical elements and that of their possible compounds. For comparison, the number of compounds synthesised is on the order of 10^6.

Minerals are grouped in classes, each of which comprises a variable number of species. In Table 2 the main classes are reported in order of decreasing number of species.

Although Al is present in 714 minerals belonging to various classes, most of it is contained in a dozen silicates and oxides–hydroxides. In Table 3 the composition and the approximate contents of Al_2O_3 of these minerals are reported.

The above formulae show Al both in tetrahedral and octahedral co-ordination: only tetrahedral Al in feldspars; only octahedral Al in kaolinite, garnets, oxides–

Table 2
The principal classes of aluminium minerals

	Class	No. of species
1	Silicates	883
2	Sulphosalts + S–Se–Te-ides	501
3	Oxides and hydroxides	392
4	Phosphates	352
5	Sulphates	293
	(Total)	2421
	Other classes	approx. 1000

Table 3
Formulae and approximate alumina contents of the most important aluminium-bearing minerals

			Al_2O_3%
Tectosilicates			
Plagioclase feldspars	Albite	$NaAlSi_3O_8$	19
	Anorthite	$CaAl_2Si_2O_8$	37
K-feldspar	Orthoclase	$KAlSi_3O_8$	19
Inosilicates			
Clinopyroxenes	Augites	$(Ca,Mg,Fe,T,Al)_2[(Si,Al)_2O_6]$	0–22
	Omphacite	$(Ca,Na)(Mg,Fe,Al)[Si_2O_6]$	1–11
	Jadeite	$NaAlSi_2O_6$	22
Amphiboles	Hornblende	$Ca_2(Mg_{4-3}Al_{1-2})[Si_{7-6}Al_{1-2}O_{22}](OH_2)$	4–13
	Hastingsite	$NaCa_2(Mg_4Al)[Si_6Al_2O_{22}](OH)_2$	
Phyllosilicates			
Micas	Biotites	$K_2(Mg,Fe)_{6-4}(Fe,Al,Ti)_{0-2}$ $[Si_{6-5}Al_{2-3}O_{20}](OH,F)_4$	11–17
	Muscovites	$K_2(Al_4)[Si_6Al_2O_{20}](OH,F)_4$	27–38
Chlorites	Clinochlore	$(Mg_{10}Al_2)[Si_6Al_2O_{20}](OH)_{16}$	10–27
	Sudoite	$Mg_4Al_6[Si_6Al_2O_{20}](OH)_{16}$	
Clay minerals	Kaolinite	$Al_4[Si_4O_{10}](OH)_8$	39
	Illites	$K_{1.5-1.0}Al_4[Si_{6.5-7.0}Al_{1.5-1.0}O_{20}](OH)_4$	27–37
	Smectites	$(Ca_{0.5},Na)_{0.7}(Al,Mg,Fe)_{4-6}$ $[(Si,Al)_8O_{20}](OH)_4.nH_2O$	variable
	Vermiculites	$(Mg,Ca)_{0.6-0.9}(Al,Mg,Fe)_6$ $[(Si,Al)_8O_{20}](OH)_4.nH_2O$	variable
Nesosilicates			
	Garnets	$(Mg,Fe,Ca)_3Al_2Si_3O_{12}$	12–25
	Kyanite, andalusite, sillimanite	Al_2SiO_5	62
Oxides-hydroxides			
	Spinel	$MgAl_2O_4$	70
	Gibbsite	$Al(OH)_3$	65
	Boehmite	$AlO(OH)$	81

hydroxides; mainly tetrahedral (jadeite, augites, hornblendes, biotites, vermiculites), mainly octahedral (omphacite, muscovite, illites, smectites), and variable (chlorites).

The minerals mentioned above are the main constituents of rocks formed in sedimentary, metamorphic and magmatic processes (Fig. 9).

Table 4 shows the most common rock types of continental and oceanic crust and their approximate contents of aluminium minerals.

From the data in Table 4 it appears that, with the exception of layer 1, the most frequent minerals are feldspars. Their compositions varies on going from basic rocks, relatively poor in silica (basalts and gabbros), to more acidic ones, with a higher silica content (granitoides), according to a general trend of decreasing Al and Ca content. Fig. 10 shows the composition range of plagioclase feldspars from albite to anorthite end-members.

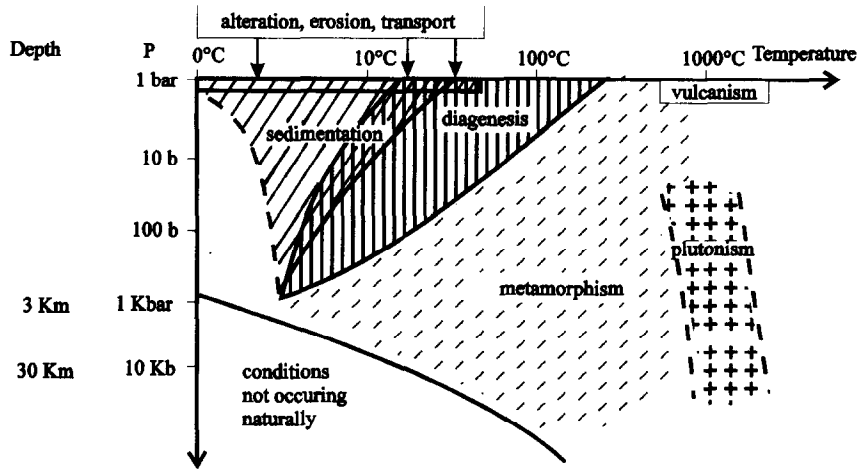

Fig. 9. Fields of the petrogenetic processes in the P–T space.

Table 4
Approximate content of aluminium-bearing minerals in the main rock types

	Rock type	Minerals	% (approx)
Upper crust, layer 1	Sediments-soils	Phyllosilicates, feldspars, hydroxides	variable
	Shales	Phyllosilicates, feldspars	variable
	Sandstones	Phyllosilicates, feldspars, inosilicates	variable
	Graywackes	Phyllosilicates, feldspars, inosilicates	variable
Upper crust, layer 2	Granodiorites	Feldspars	50
		Phyllosilicates	10
		Inosilicates	5
	Gabbros	Feldspars	50–60
		Inosilicates	40–50
	Paragneiss-schists	Feldspars	variable
		Phyllosilicates	variable
		Inosilicates	variable
Lower crust	Granulites	Feldspars	variable
		Inosilicates	variable
		Garnet	variable
Oceanic crust	Basalts	Feldspars	45
		Inosilicates	25
		Volcanic glass	25

The covariance of the four oxides depends on the heterovalent substitution

$$Na^{+}\ Si^{4+} \rightleftharpoons Ca^{2+}\ Al^{3+}$$

albite anorthite

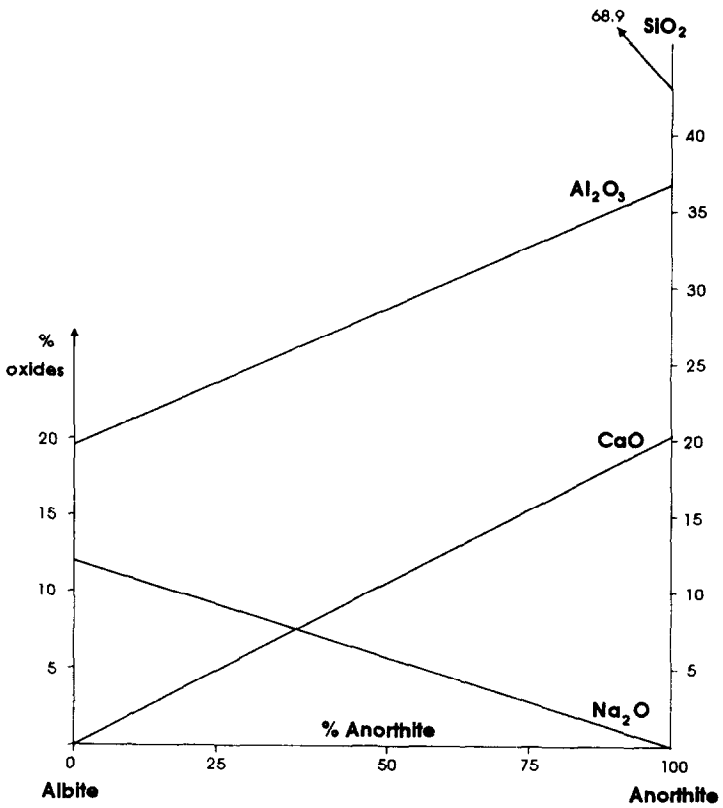

Fig. 10. Chemical composition of the plagioclase series.

and is bound to the tetrahedral occupancy (Si,Al)–O typical of aluminosilicates.

From a knowledge of the percentage of anorthite (which can be rapidly estimated by microscopic observation of a thin slide of rock under polarised light) we can obtain the Al_2O_3 content (Fig. 10). Moreover, by estimating from an optical examination the modal abundance of plagioclase, we can compute the amount of Al_2O_3 it contributes to the rock. Although the same method can also be applied to evaluate the amount of the other minerals present in the rock, it is not generally possible to measure their Al_2O_3 contribution as in the case of plagioclase; however, if their alumina content can be estimated by other means it is possible to compute also their contribution to the total Al_2O_3 budget of the rock.

The above procedure can be illustrated by applying it to a granodiorite and to a basalt, the mineralogical and chemical characters of which are representative of the upper crust and of the oceanic crust, respectively (Table 5).

The above data stress the (dominating) contribution of feldspars to the total budget of alumina in magmatic and metamorphic rocks. The feldspars can exert the same role in sedimentary rocks, if their terrigeneous minerals derive from the above

Table 5
Estimation of the Al_2O_3 percentage contributed by different minerals according to their aluminium content and their modal frequence in two typical rocks

Minerals	% of Al_2O_3 in the mineral	% modal frequence of the mineral	% (Al_2O_3) contributed
Granodiorite			
Plagioclase (An_{30})	26	48	12.5
K-feldspar (Or_{90})	18	10	1.8
Biotite	15	6	0.9
Hornblende	9	6	0.5
Bulk-rock	16.2		tot. 15.7
Basalt			
Plagioclase (An_{60})	30	45	13.5
Clinopyroxene	6	25	1.5
Volcanic glass	variable	27	—
Bulk-rock	17		tot. 15

crystalline rocks. However, if the feldspars in the sedimentary process strongly suffered chemical transformations, their role fails because other minerals, as phyllosilicates and hydroxides, become the main carriers of aluminium. As we will see, clay phyllosilicates and hydroxides are formed mainly from altered feldspars, which are therefore the main source of crustal aluminium: directly in cristalline rocks; more or less indirectly in sedimentary ones.

3.3.3. The distribution of aluminium in sedimentary rocks

As shown in Fig. 9, the temperature and pressure conditions prevailing in the sedimentary process are less severe than in the formation of metamorphic and magmatic crystalline rocks. The latter come from the solidification of magmas, either in depth (plutonic) or at the surface (volcanic); the former are produced by the recrystallisation in subsolidus conditions of preexisting rocks. The formation of sedimentary rocks begins with the physical and chemical breakdown of preexisting rocks. Disintegration and decomposition of rocks are intimately related, but here are stressed some aspect of chemical weathering. This results from the adjustment of thermodynamically unstable minerals to the surface environment of abundant water and atmospheric gases. Of the main chemical processes (solvation, solution, hydrolysis, ion exchange, oxidation, organic reaction) hydrolysis is the most important for the generally scarcely soluble silicate rocks. Of the common rock forming Al-minerals above mentioned, the susceptibility to weathering increases from the K-feldspar to sodic-intermediate and calcic plagioclase, and from muscovite to biotite, then hornblende–pyroxene, according to the scale of Goldich. A hydrolysis reaction as: mineral + water⟶ products is better indicated taking into account the presence of dissolved carbon dioxide in natural waters. Thus hydrolysis of the main

rock forming mineral such as the feldspars is of the type

$$H_2O + CO_2 \leftrightharpoons H_2CO_3$$

$$4(Na,K)AlSi_3O_8 + 4(H^+ + HCO_3^-) + 18H_2O \rightarrow$$

$$\rightarrow 4(Na,K)^+ + 4HCO_3^- + 8H_4SiO_4 + Al_4(OH)_8SiO_{10}$$

The significant consequences of this reaction are:

- liberation of cations;
- production of the bicarbonate anion (the dominant ion in fresh waters);
- basification of the resulting solution since the silicic acid molecules ties up some H^+ of the water;
- production of Al minerals (phyllosilicates or hydroxides).

The neoformation of aluminium minerals and amorphous compounds ultimately depends on the following.

(a) Release of Al ions from the lattice of weathered minerals.

(b) Formation of octahedrally co-ordinated aquo-aluminium ions $Al(H_2O)_6^{3+}$ followed by deprotonation to monomer $AlOH(H_2O)_5^{2+}$; then by formation of the dimer $Al_2(OH)_2(H_2O)_8^{4+}$ and then larger units to form chains. If three dimeric ions are further deprotonated, the double OH bridges might be shared giving a branched chain, formula $Al_6(OH)_8(H_2O)_{16}^{8+}$, containing a central aluminium ion co-ordinated by six OH ions. The coalescence of these octahedral units by sharing three independent edges produces a sheet of hexagonal rings, as shown by Fig. 11. This structure typical of the gibbsite is an integral part of dioctahedral Al phyllosilicates. The relative proportions of the different species depend on the conditions during the hydrolysis (pH value, Al-concentration and age of hydrolysis products). However, under equilibrium constraints polynuclear hydroxyaluminium ions would be considered as unstable, transient species on the way to becoming solid $Al(OH)_3$.

(c) Formation of silicoaluminum copolymers, evolving to clays and silica layers alternate in various ways (Fig. 11); the solubiity of silica is a complementary factor in the speciation of aluminium minerals.

An important factor in weathering is the water flow. At moderate flow, kaolinite forms; whereas, at very low flow the poor leaching of ions allow the formation of smectites and illites. Vice versa, for high rates of flow all the cations and silicic acid are removed fast enough to allow hydroxides of Al to form; this is the why bauxite minerals such as gibbsite and boehmite tend to form in areas of high rainfall and high relief favoring water percolation through soils and bedrock. Other relevant factors are the mineralogy of the rock to be weathered and the composition renewal of weathering solutions; high production of H^+ (e.g. by decay of organic matter or oxidation of sulphides) accelerate the weathering processes.

A graphical method showing stability relations of the products originating from the feldspars alteration is based on the activity–activity diagrams. Fig. 12 show the case of albite weathering. Decreasing of Na activity with increasing H^+ favours the formation of gibbsite when the silica concentration is very low; with increasing activity of dissolved silica, kaolinite is more stable than gibbsite and Na-smectite is more stable than kaolinite. Similar diagrams define the stability fields of Ca-smectites

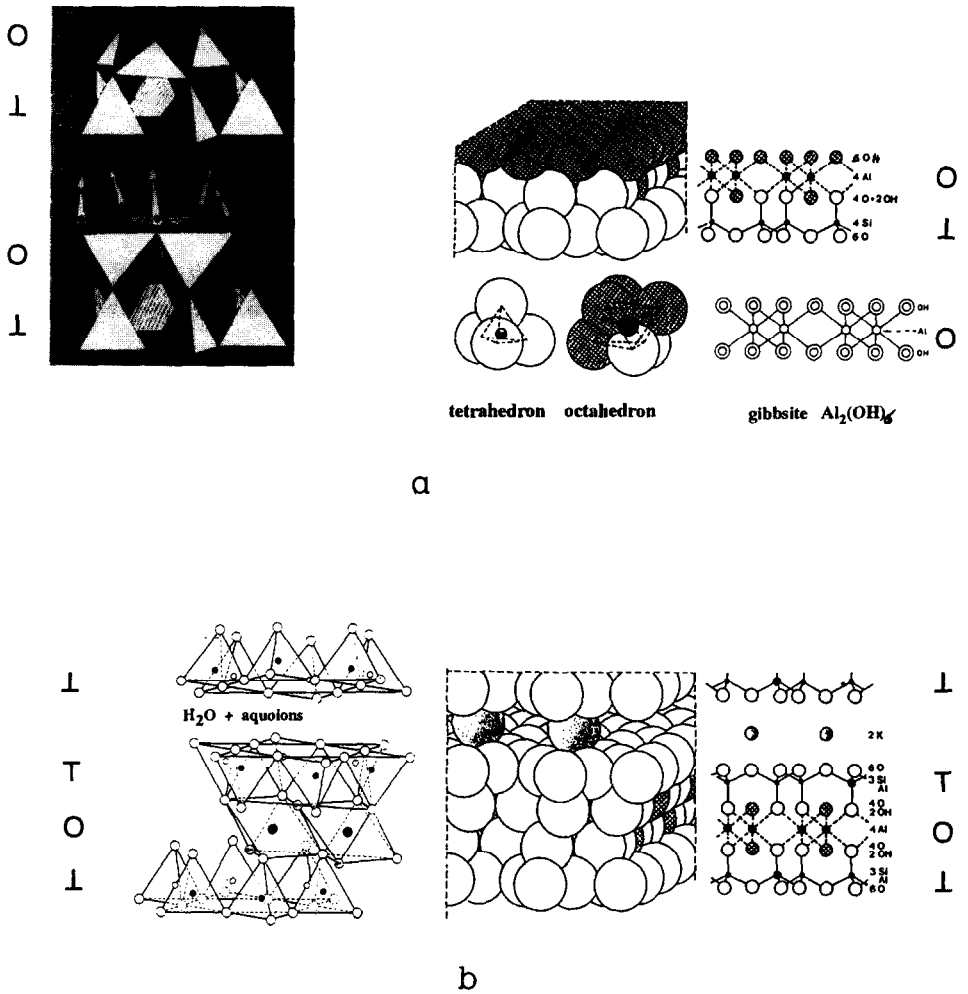

Fig. 11. (a) Scheme of the crystal structure of kaolinite. Linked silica tetrahedra form the tetrahedral sheets (T); linked octahedra of gibbsite form octahedral sheets (O). Repeated units of one tetrahedral sheet and one octahedral sheet build up the T–O or 1:1 layer. (b) Scheme of the crystal structure of muscovite–illite and smectite. A gibbsite sheet between two tetrahedral sheets form a T–O–T or 2:1 layer. Aluminium may substitute for silicon in tetrahedral sheets and various cations may substitute for aluminium in the octahedral sheet. Because of the substitutions, deficiency of positive charges is balanced by interlayer potassium in the muscovite–illite and aquoions in smectites. The reversed T indicate that apex oxygen in tetrahedra are oriented upwards.

and K-smectites and illites produced by the weathering of Ca-plagioclase and K-feldspar, respectively. The general relationships shown by these diagrams agree with those found in nature. An interesting use of the above diagrams is to plot analyses of the various natural waters. Most fresh waters are supersaturated with

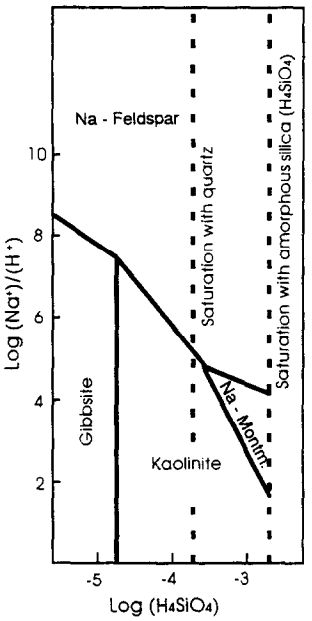

Fig. 12. Activity–activity diagram showing stability relations in the system Na_2O– Al_2O_3–H_2O. (After Ref. [12]).

respect to quartz but not relative to amorphous silica and plot in the field of kaolinite which is the major Al-mineral produced by chemical weathering.

A complementary and expressive graphical method to illustrate the extent of the weathering, uses the apparent variations of the percentage of Al_2O_3 vs. the proportions of minerals forming the altered rock (Fig. 13). Since Al-hydroxides are practically insoluble within the pH range of natural water (solubility less than 1 ppm at pH 6–8 in pure water), Al tend to remain at a weathering site in the form of clay or hydroxide mineral. A relative increase of Al_2O_3 thus results because of the leaching of the oxides released from the labile biotite, inosilicates, feldspars, etc.; if even the silica tend to be removed, the only minerals resulting are Al hydroxides and eventually Fe oxide–hydroxides, both typically associated in the lateritic soils occurring in areas with high water-flow rates.

Ultimately the Al–clay minerals (with more or less hydroxides) are the major products of the main type of sedimentary rocks, i.e. the shales. The average Al_2O_3 figures in the common sedimentary rocks are around 15% in the shales, 13% in the graywackes, 5% in the sandstones and 1%–2% in the carbonate rocks.

All these rock types are combinations of minerals that survive weathering and transportation (detrital minerals, as quartz), new minerals formed during weathering and transportation (secondary minerals, as clay shales), minerals that form directly from solutions (precipitated minerals, as carbonate) and minerals formed in sediments during and after deposition (authigenic minerals, as clay and carbonate minerals). The possibility of different proportion of detrital, secondary, precipitated and authi-

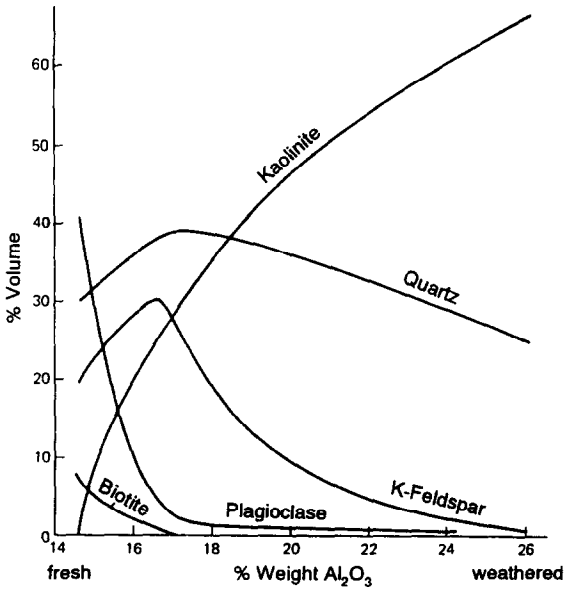

Fig. 13. Mineral-variation diagram for the weathering of granitic gneiss. Wt.% Al_2O_3 is used as a measure of the extent of weathering of fresh rock on the left to final soil on the right. (After Goldich, J. Geol., 46 (1938)).

genic phases produces a wide range of chemical compositions in the sedimentary rocks, sediments and soils.

It has been found that, with a decrease in grain size, aluminium (as iron) tends to increase due to a decrease in quartz abundance and an increase in clay minerals. Thus, for comparative purposes, the chemical composition of rocks of similar grain size should be considered. Shales, owing the predominance of clay minerals on the minor quartz, have a relative uniformity in size and in the ratio of the two main oxides, SiO_2 and Al_2O_3. On a plot of log (SiO_2/ Al_2O_3) vs. log (($CaO + Na_2O$)/K_2O) the average composition of shales is close to the average composition of igneous rocks.

Because of adsorption or ion exchange occurring on clay minerals surfaces (see below), shales clearly have higher amounts of most trace elements when compared with other sedimentary rocks. Among the trace, RRE and Th as incompatible, Sc as compatible elements are of particular interest. In fact they are practically insoluble in natural waters, where they have very short residence time (in this resembling Al and Fe^{III}); thus they are transferred virtually quantitatively into terrigenous clastic sedimentary sequences. For such chemical and physical features, shales and the particulate matter of big rivers are taken to be representative of the upper crust. Post-Archean clastic sedimentary REE patterns differ from the more variable Archean patterns; further, post-Archean sedimentary rocks have higher Th/Sc and La/Sc ratios and lower La/Th ratios.

The uniform distribution of REE in the shales and particulate material of some

rivers is shown in Fig. 14. The upper crustal REE pattern provide a guide for evaluating the abundance levels of other elements; the pattern is close to that of typical granodiorite, which most other studies suggest to be close to the average composition of the upper crust (Fig. 5 and Table 1).

Significantly, Al_2O_3 ranges 16%–24% in typical Australian post-Archean shales and 16%–25% in big rivers as the Amazon (23%), Congo (25%), Ganges (25%), Garonne (22%) and Mekong (22%).

Estimates of global averages of the dissolved, suspended, and wind-blown loads carried from the continents are [3]

dissolved load in rivers (2.5×10^{15} g y^{-1})

suspended load in rivers (6.5×10^{15} g y^{-1})

wind-blown load in rivers (1.0×10^{15} g y^{-1})

total (10.0×10^{15} g y^{-1})

This annual discharge from continental crust to ocean is of the same order of the annual production of basaltic magmas at the ocean ridges (20 km^3 y^{-1}, i.e. about 60×10^{15} g y^{-1}). The mass ratio of the loads dissolved/suspended is 1/2.6. Of the total mass of crustal rocks that is being weathered, the mass fraction going into solution annually is $1/(1+2.6)=0.28$ or about 30%; the remaining 70% of the weathered products are carried as solids. Assuming a river flow of 3.2×10^{19} g y^{-1} the preceding estimates correspond to an average concentration of about 80 mg l^{-1} of dissolved and 200 mg l^{-1} of suspended material.

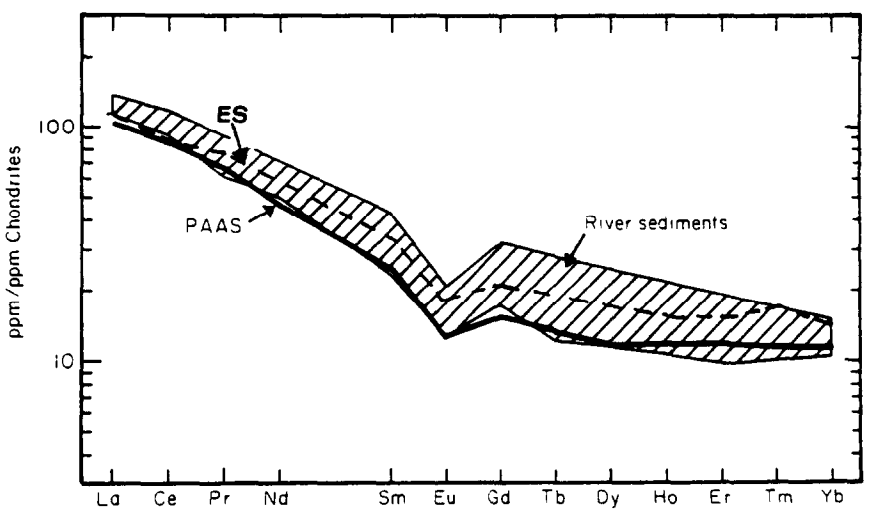

Fig. 14. Chondrite-normalized diagram of post-Archean shale composites (PAAS, ES) and modern river sediments. The uniformity of the patterns support the view that sedimentary REE patterns reflect the upper continental crust exposed to weathering and erosion. Such patterns would best compare to granodioritic composition. (After Ref. [4], modified).

The average concentration of Al in river water is 5×10^{-8} g g^{-1} or 5×10^{-2} mg l^{-1} whereas in ocean water it is 8×10^{-8} g g^{-1} [4]. From the above data, Al represents only 1/600 of the dissolved load whereas Al in the suspended load is 20 mg l^{-1}/200 mg l^{-1}, i.e. 1/10. So the Al suspended/Al dissolved ratio is ca. 400. In other words, Al delivered by the weathered crust enters the aqueous environment largely as particulate matter of clay minerals, hydroxides and colloids; the dissolved form of inorganic monomeric aluminium is less than a few micromoles per litre in the normal pH range of river water (6–8). This is also the pH range of minor solubility experimentally measured for $Al(OH)_3$.

Any discussion on the concentration and forms of aluminium in natural waters should require ability to differentiate precisely and accurately between aqueous and particulate aluminium, as well as between inorganic and organic forms of aqueous aluminium. Because particulate materials exhibit a continuous size distribution, no absolute distinction between dissolved and suspended forms can be made and results show a strong dependence on the operational procedures.

Exhaustive insights on the most fundamental aspects of Al chemistry in the environment are given in Ref. [5]. Various topics as quantitation of Al in soils, stable chemical forms both as dissolved solute and as solid phase, polynuclear and colloidal hydrolytic species in aqueous solution, Al-complexes with natural organic ligands, surface reaction as both adsorptive and adsorbent, spatial and temporal variability, metastability, are widely discussed through more than 300 pages.

Among the arguments mentioned we recall the one regarding surface reactivity of the main Al-carriers, i.e. clay-hydroxides minerals and colloids. On decreasing the particle size the specific area increases and in some phyllosilicates, as montmorillonite and vermiculites, it can attain 700–800 m^2 g^{-1}. Certainly, the fact that surfaces of soil particles are extensive and reactive lead to a dominance of surface chemistry in soil behaviour. It has been suggested that the relationships of surface chemistry to soil science is similar to that of biochemistry to biology.

The surfaces of clay particles often differ from the constitution which might be expected from their internal structures because of strongly adsorbed materials normally present on those surfaces.

In clay particles of the 2 : 1 lattice type the siloxane surface predominates, composed of quasi planar oxygen ions underlain by silicon ions (Fig. 11). They are dominated by negative charges arising from isomorphous substitution in tetrahedral and/or octahedral sheets; their hydration depends on the interaction between the exchange cations and water molecules, with only weak hydrogen bonds between water and surface oxygens. On the broken edges of these phyllosilicates and in the alternate sheets of gibbsite of kaolinites– chlorites, the surface is of silanol Si–OH and aluminol Al–OH, i.e. of hydroxide M–OH type where M represents a co-ordinated metal.

The charge of the hydroxide surface arises from association or dissociation of protons

$$M{-}OH_2^+ \overset{H^+}{\rightleftharpoons} M{-}OH \overset{OH^-}{\rightleftharpoons} M{-}O^- + H_2O$$

The extent of protonation–deprotonation depends on the concentration of protons

near the surface, and hence on pH and electrolyte concentration of the soil solution. The pH at which the surface is uncharged is known as the point of zero charge, and reflects the affinity at the M^{n+} ion for electrons; the point of zero charge of Al_2O_3 is between 7.5 and 9.5. However, oxide surface tends to hydrate readily so that in wet conditions common in the soils the oxides of Al (corundum), Fe^{III} (hematite) and Si (quartz) are hydrated as $Al(OH)_3$ (gibbsite), FeOOH (goethite) and H_4SiO_4 (silica gel). The surface hydroxides are directly bound to metal ions and the adsorbed water becomes hydrogen bonded to them; the hydrophylicity of hydroxide surfaces is lacking in the inert oxygen of the siloxane surface.

The different behaviour of siloxane and hydroxide surfaces is apparent in Fig. 15. The positive charges of gibbsite and goethite are due to protonation of the surface hydroxyls below the point of zero charge and to deprotonation above it. The nearly constant negative charge of the smectite is independent of pH, cation and electrolyte concentration.

An important aspect of the hydrous oxides of Al is the participation in ligand exchange reactions with cations and anions. The chemiadsorbed ions can substantially modify the surface properties.

Hydroxy–Al polymers can drastically reduce the cation exchange capacity (CEC) of many soil clays, especially Na-montmorillonites, and affect the selectivity of various ions and modify the collapse of the clay layers. So, the moisture-retention properties and aggregate properties of clays and soils can be generally affected by the adsorption of Al species; for instance, the structure of lateritic soils is improved through the interaction of positive Al hydroxides with the negative charges of other soil components.

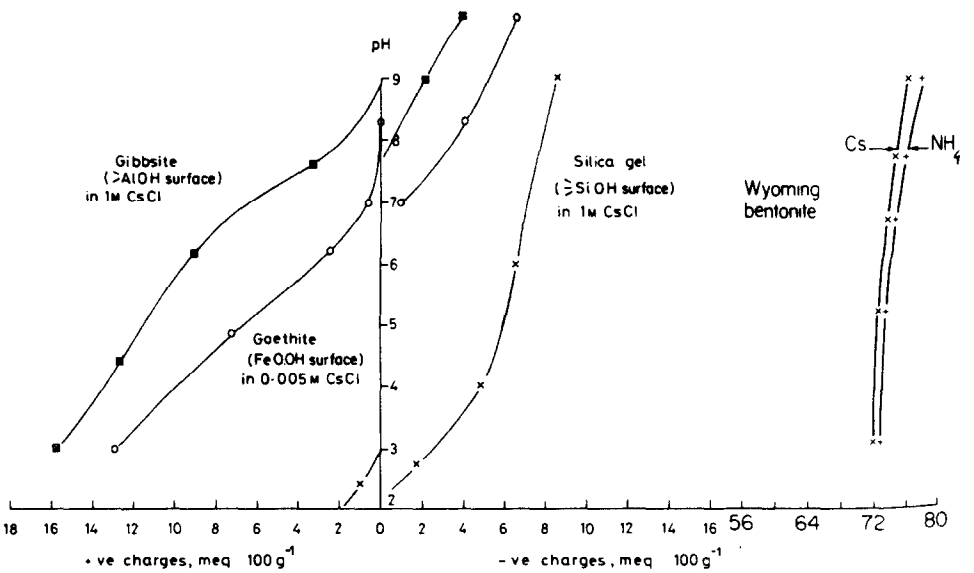

Fig. 15. Charges on gibbsite, goethite, silica and bentonite surfaces in the pH range 3–9. (After Ref. [6]).

The role of Al species in controlling geochemical and geotechnical properties and phenomena is widely discussed in Refs. [6–8].

A topic of increasing interest regards the sorption interactions between the clay minerals and organic compounds with the formation of stable complexes between clay minerals or humic compounds and various enzymes (mostly of microbial origin). It has been determined that the surface of clay minerals not only protects these unstable substances from rapid decay, but that it can catalytically act upon the transformation and polymerisation of various organic compounds, including aminoacids and their derivatives. The discoveries and continuing deeper knowledge of these catalytic properties of clay minerals in interaction with organic substances support the hypothesis that the pre-biotic formation of biological polymers took place on mineral surfaces: these polymers may have been the precursors of the RNA world [9].

3.4. Ores and economic geology of aluminium

The mordant properties of a natural substance called alumen have been known for a very long time: Plinius the Elder knew the mineral, which was extracted near Rome. This substance, $K_2SO_4 \cdot Al_2(SO_4)_3 \cdot 24H_2O$, now called alunite, gave the name to aluminium. The first aluminium ingot was prepared in 1854, and since 1886 the process based on the electrolysis of Na_3AlCl_6 in the presence of a flux (first fluorite and then cryolite) was superseded by the electrolysis of alumina dissolved in molten cryolite. For a recent review on aluminium metallurgy see Ref. [10].

The production of metal increased from 7 Gg y^{-1} in 1900 to 16000 Gg y^{-1} in 1980. During 1986 the main producers of bauxite were Australia ($\approx$32000 Gg), Guinee ($\approx$15000 Gg), Jamaica, Russia, Brazil (6–7000 Gg each), Surinam (3700 Gg), France (1300 Gg).

Almost the totality of Al is produced from bauxite; small amounts come from alunite (16%–18% Al_2O_3) and from nepheline (25%–30% Al_2O_3); the extraction of the metal from clay is still not economical. The main elements present in bauxites, besides Al, O and H, are Fe, Si and Ti; to be exploited, bauxites must contain less than 8% silica, while iron content is less critical. Generally, useful deposits must contain more than 40% Al_2O_3. Bauxite is found mostly in cretaceous–quaternary rocks, while supporting rocks may be even pre-cambrian; most deposits lie in the equatorial belt. As in geological times the position of the poles has changed, thus shifting the climatic zones, there has been a global oscillating evolution of the weathering crust and continental sediments. The tectonic evolution of continents also played an important role. Plants, which exert a substantial influence on weathering processes, and hence on the formation of the crust, appeared on the continents only from Devonian. The substances produced by continental plants during their life, and released after their extinction, are taken down by rain water and contribute to its acid reaction in the initial stage of infiltration into the rocks. The migration of the continents explains why bauxite deposits can be found also outside the present equatorial belt (Fig. 16).

Bauxite deposits are hosted in carbonate or silicate rocks; in the first, the mineral is often found inside karsic cavities or overlaid on a more or less calcified carbonate

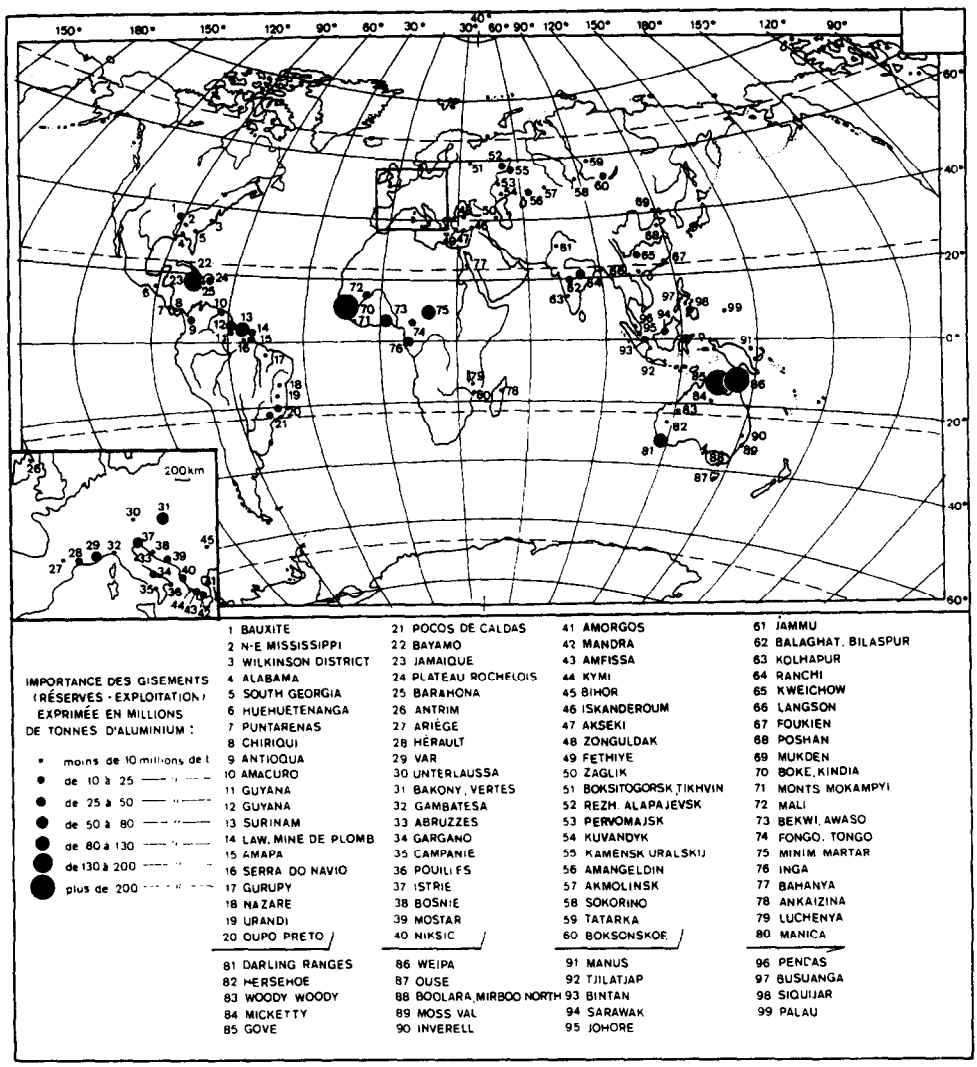

Fig. 16. Principal Al ore deposit in the world. (After Ref. [13].)

substrate, where it was transported from more or less distant zones. These rocks contain mainly boehmite, associated with gibbsite and diaspore, and were the only source of aluminium in the first part of this century. At the present time the mineral comes mainly from deposits in silicate rocks. These come from the weathering of parent rocks more or less rich in feldspars or feldspathoids and may be autochthonous (Brazil, Guyana, Australia) or reworked and enriched in Al owing to subsequent climatic modifications (Cape York, Australia). These bauxites are generally found in cratonized areas subjected to continental alteration. The most abundant mineral is

gibbsite, with minor amounts of boehmite, kaolinite and oxides of iron, titanium and manganese.

References

[1] G.J.MacPherson, A.M. Davis and E.K.Zinner, The distribution of aluminium-26 in the early Solar System-A reappraisal, Meteoritics, 30(4) (1995).
[2] A.S. Marfunin, Advanced Mineralogy, Vol. 1, Springer, Berlin, 1994.
[3] A. Lerman, Geochemical Processes, Wiley, New York, 1979.
[4] S.R. Taylor and S.M. McLennan, The Continental Crust: its Composition and Evolution, Blackwell Scientific, Oxford, 1985.
[5] G. Sposito, The Environmental Chemistry of Aluminum, CRC Press, Boca Raton, 1989.
[6] D.J. Greenland and M.H. Hayes, The Chemistry of Soil Constituents, Wiley, New York, 1978.
[7] D.J. Greenland and M.H.B. Hayes, The Chemistry of Soil Processes, Wiley, New York, 1981.
[8] J.K. Mitchell, Fundamental of Soil Behavior, Wiley, New York, 1993.
[9] J.P. Ferris, The Chemistry of Life's Origins, Kluwer, Dordrecht, 1993.
[10] J. Castle, Advances in the extractive metallurgy of aluminium, Mining Magazine, August 1995.
[11] G.C. Brown and A.E. Mussett, The Inaccessible Earth, Chapman and Hall, London, 1993.
[12] W. Stumm and J.J. Morgan, Aquatic Chemistry, Wiley, New York, 1981.
[13] P. Niccolini, Gitologie et Exploration Minire, Tec. and Doc. Lavoisier, Paris, 1990.
[14] T. Encrenaz, J.P. Bibring and M. Blanc, The Solar System, Springer, Berlin, 1990.
[15] U.G. Jorgensen, Molecules in the Stellar Environment, Springer, Berlin, 1994.
[16] S.F. Mason, Chemical Evolution, Clarendon, Oxford, 1992.
[17] N. Prantzos, E. Vangioni-Flam and M. Cass, Origin and Evolution of the Elements, Cambridge University Press, Cambridge, 1993.